

Supplementary Information for “*Ab Initio* Study of Electron and Hole Transport in Pure and Doped MnO and MnO:ZnO Alloy”

Dalal K. Kanan¹ and Emily A. Carter²

*Departments of ¹Chemistry and ²Mechanical and Aerospace Engineering,
 Program in Applied and Computational Mathematics, and Andlinger Center for
 Energy and the Environment, Princeton University, Princeton, NJ 08544-5263*

A. Computational details

Cluster models used in this study listed according to pathway and material

Table S1. Clusters used to model the hole transport pathways in the materials under consideration

Material	Hole Transport Pathway	Clusters
Undoped MnO	Mn ↔ Mn Mn ↔ O O ↔ O	[Mn ₂ O ₁₀] ¹⁵⁻ , [Mn ₄ O ₁₈] ²⁷⁻ , [Mn ₆ O ₂₂] ³¹⁻
Undoped MnO:ZnO	Mn ↔ Mn Mn ↔ O O ↔ O	[MnZnO ₁₀] ¹⁵⁻ , [Mn ₂ ZnO ₁₃] ¹⁹⁻ , [Mn ₂ Zn ₂ O ₁₈] ²⁷⁻ , [Mn ₃ ZnO ₁₈] ²⁷⁻ , [Mn ₅ ZnO ₂₂] ³¹⁻
Doped MnO and MnO:ZnO	Mn ↔ Mn Mn ↔ O O ↔ O	[MnLiO ₁₀] ¹⁶⁻ , [Mn ₂ LiO ₁₃] ²⁰⁻ , [Mn ₃ LiO ₁₈] ²⁸⁻ , [Mn ₅ LiO ₂₂] ³²⁻

Table S2. Clusters used to model electron transport pathways in the materials under consideration

Material	Electron Transport Pathway	Clusters
Undoped MnO	Mn ↔ Mn	[Mn ₂ O ₁₀] ¹⁷⁻
Doped MnO	Mn ↔ Mn	[Mn ₂ GaO ₁₃] ²⁰⁻
	Mn ↔ dopant	[MnGaO ₁₀] ¹⁶⁻
Undoped MnO:ZnO	Zn ↔ Zn	[Zn ₂ O ₁₀] ¹⁷⁻ , [Zn ₃ O ₁₄] ²³⁻ , [Zn ₄ O ₁₈] ²⁹⁻ , [Zn ₄ O ₁₆] ²⁵⁻ , [Zn ₆ O ₂₂] ³³⁻ , [Zn ₁₀ O ₂₈] ³⁷⁻ , [Zn ₅ MnO ₂₂] ³³⁻ , [Zn ₄ Mn ₂ O ₂₂] ³³⁻ , [Zn ₃ Mn ₃ O ₂₂] ³³⁻ , [Zn ₂ Mn ₄ O ₂₂] ³³⁻ , [Zn ₃ MnO ₁₈] ²⁹⁻ , [Zn ₂ Mn ₂ O ₁₈] ²⁹⁻
	Zn ↔ Mn	[ZnMnO ₁₀] ¹⁷⁻
Doped MnO:ZnO (with <i>M</i> = Al, Sc, Ti, Ga, Y, In, Sb, Gd)	Zn ↔ Zn	[Zn ₂ FO ₉] ¹⁶⁻ , [Zn ₆ FO ₂₁] ³²⁻ , [Zn ₅ MO ₂₂] ³²⁻
	Zn ↔ dopant	[ZnMO ₁₀] ¹⁶⁻

Basis set contractions

The Mn and O basis sets were contracted as $7s6p7d \rightarrow 2s2p4d$ and $5s5p1d \rightarrow 3s3p1d$, respectively, following earlier work that showed this contraction gives accurate results for excitation energies compared to all-electron basis sets.¹ The F basis set was contracted as $5s5p1d \rightarrow 3s3p1d$. The Gd basis was left uncontracted to obtain accurate geometries. The remaining basis set contractions were obtained from the references within the main text.

B. Hole transport in Li-doped MnO

We considered the effect of Li symmetrically positioned relative to Mn \leftrightarrow Mn and O \leftrightarrow O hole transfer (Table 1). The Mn \leftrightarrow Mn hole transfer barrier is ~ 0.8 eV (in $[\text{Mn}_2\text{LiO}_{13}]^{20-}$ and $[\text{Mn}_5\text{LiO}_{22}]^{32-}$) and the O \leftrightarrow O barrier is $\sim 0.4 - 0.5$ eV (in $[\text{MnLiO}_{10}]^{16-}$ and $[\text{Mn}_3\text{LiO}_{18}]^{28-}$). Thus, Li has a negligible effect on O \leftrightarrow O or Mn \leftrightarrow Mn hole transfer barriers compared to undoped MnO.

We then studied the effect of Li asymmetrically located relative to Mn \leftrightarrow Mn hole transfer in $[\text{Mn}_3\text{LiO}_{18}]^{28-}$. We find a 0.79 eV barrier for $\text{Mn}_{\text{near}} \rightarrow \text{Mn}_{\text{far}}$ transfer, while the reverse barrier is 0.15 eV. A hole transferring along the Mn \leftrightarrow Mn pathway away from Li encounters a barrier (0.79 eV) similar to the undoped case (0.77 eV in $[\text{Mn}_4\text{O}_{18}]^{27-}$).

For Li asymmetrically located with respect to O \leftrightarrow O hole transfer, the hole slightly prefers (by 0.09 eV) to localize on the O closer to Li compared to the O farther away. The $\text{O}_{\text{near}} \rightarrow \text{O}_{\text{far}}$ barrier is 0.46 eV while the reverse barrier is 0.37 eV (in $[\text{Mn}_5\text{LiO}_{22}]^{32-}$). A hole transferring along the O \leftrightarrow O pathway away from Li encounters a barrier (0.46 eV) similar to the comparable undoped case (0.38 eV). Thus, Li does not convert nearby O ions to trap sites and negligibly affects the barrier for O \leftrightarrow O hole transfer barrier.

¹ Kanan, D. K.; Carter, E. A. *submitted*.

C. Hole transport in MnO:ZnO occurs via hopping among and between Mn and O ions, with little influence from Zn

When Zn is asymmetrically placed with respect to donor/acceptor Mn atoms (in $[\text{Mn}_3\text{ZnO}_{18}]^{27-}$; Figure 3), the hole prefers to reside on the Mn closer to Zn by only 0.02 eV (Table 1). When Zn is asymmetrically placed with respect to donor/acceptor O atoms (in $[\text{Mn}_5\text{ZnO}_{22}]^{31-}$), the hole prefers to be on the O farther away from Zn by only 0.03 eV. Moreover, the barriers computed for the Mn \leftrightarrow O pathways are all very similar regardless whether the O is situated near to or far from a Zn atom. These small variations show Zn has little effect on hole transfer in MnO:ZnO.

D. Electron transport in MnO:ZnO occurs via hopping among Zn ions with little influence from Mn

We also studied the $[\text{Zn}_6\text{O}_{22}]^{33-}$ cluster with increasing substitutions of Mn for spectator Zn atoms. This allows us to explicitly explore the effect of Mn alloying on Zn \leftrightarrow Zn electron transfer (see Figure 4 for cluster depictions). In all cases, Mn alloying changed the barrier by < 0.1 eV compared to the Zn_xO_y cluster of the same size (Table 5). In $[\text{Zn}_3\text{MnO}_{18}]^{29-}$, the electron shows a slight preference (by only 0.08 eV) for residing on the Zn closer to Mn than the one farther away. The barrier from $\text{Zn}_{\text{near}} \rightarrow \text{Zn}_{\text{far}}$ is 0.61 eV, again showing that Mn has little effect on the Zn \leftrightarrow Zn electron transfer barrier. Thus, geometric changes in the model (*i.e.*, cluster shape and size) affect the barrier more than differences in the spectator atoms' electronic structure (*i.e.*, Zn^{2+} vs. Mn^{2+}).

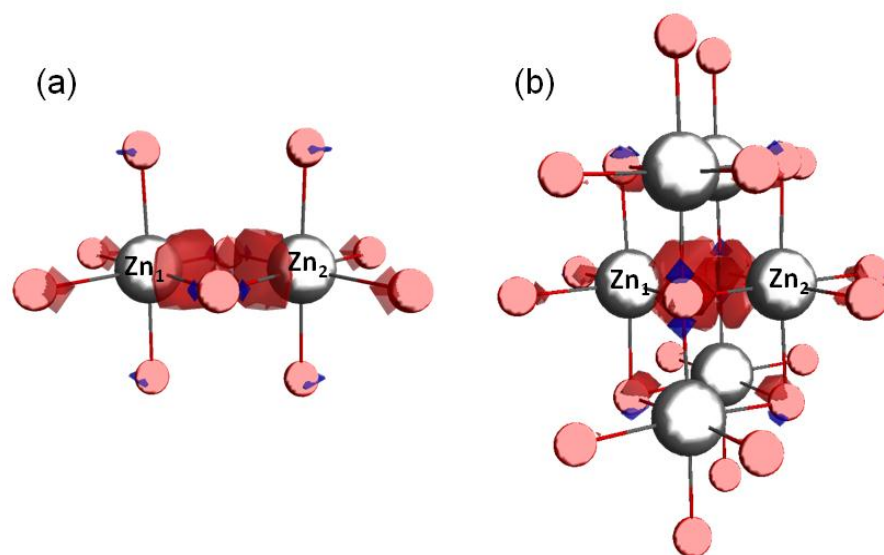


Figure S1: Density difference isosurfaces for an electron added to (a) $[\text{Zn}_2\text{O}_{10}]^{17-}$ and (b) $[\text{Zn}_6\text{O}_{22}]^{33-}$ at the crossing point geometry. An isosurface value of $0.03 \text{ electrons}/\text{\AA}^3$ is used. The difference is taken for the cluster density with the itinerant electron minus the cluster density without it; see text for details. Red (blue) indicates increased (decreased) electron density in the cluster with the electron relative to the cluster without it. Pink and white spheres denote O and Zn ions, respectively. The delocalized nature of the electron between Zn_1 and Zn_2 is evident.

E. Additional details for *n*-type doping in MnO:ZnO

Ga is an unfavorable dopant choice. When Ga and Zn reside in face-sharing octahedra (in $[\text{ZnGaO}_{10}]^{16-}$), Ga ions form deep trap states with a 1.49 eV barrier for $\text{Ga} \rightarrow \text{Zn}$ electron transfer (Table 4 and Figure 8(c)). Meanwhile, the barrier for the reverse process is only 0.21 eV and $\Delta G^0 = 1.28 \text{ eV}$. Consequently, electrons transferring via the $\text{Zn} \leftrightarrow \text{Zn}$ pathway are trapped by Ga just as in pure MnO (Table 3). When Ga and Zn reside in edge-sharing octahedra and are 40% farther away than in the previous model, the $\text{Ga} \rightarrow \text{Zn}$ and $\text{Zn} \rightarrow \text{Ga}$ barriers are 1.28 and 0.56 eV, respectively (for $[\text{Zn}_5\text{GaO}_{22}]^{32-}$; Table 4). The corresponding ΔG^0 is 0.72 eV. Therefore, Ga acts as an electron trap in both cases regardless of the electron transfer distance. We also assessed the effect of Ga on $\text{Zn} \leftrightarrow \text{Zn}$ electron transfer. The presence of Ga in $[\text{Zn}_5\text{GaO}_{22}]^{32-}$ only slightly affects the $\text{Zn} \leftrightarrow \text{Zn}$ electron hopping barrier (Table S3). Electron transfer from $\text{Zn}_{\text{edge-sharing}} \rightarrow \text{Zn}_{\text{face-sharing}}$ requires overcoming a 0.21 eV barrier while the reverse

process is completely downhill. This indicates the electron more favorably localizes on the Zn slightly farther away from Ga.

Indium doping exhibits less dramatic trapping than Ga with $\Delta G^0 = 0.47$ eV (Table 4). The Zn \leftrightarrow Zn electron transfer barrier in the presence of a spectator In atom in $[\text{Zn}_5\text{InO}_{22}]^{32-}$ changes very little. E_a^* for electron transfer from the edge-sharing Zn to the face-sharing one is 0.14 eV. E_a^* for the reverse process is 0.20 eV (Table S3).

Table S3: E_a^* and ΔG^0 for electron transfer in doped MnO:ZnO (eV). A negative ΔG^0 indicates a larger driving force for electrons to localize on $\text{Zn}_{\text{face-sharing}}$ (see text for details).

Material	Cluster model ^a	$\text{Zn}_{\text{edge-sharing}} \rightarrow \text{Zn}_{\text{face-sharing}}$	$\text{Zn}_{\text{face-sharing}} \rightarrow \text{Zn}_{\text{edge-sharing}}$	ΔG^0
Ga-doped	$[\text{Zn}_5\text{GaO}_{22}]^{32-}$	0.21	0.00	0.21
In-doped	$[\text{Zn}_5\text{InO}_{22}]^{32-}$	0.14	0.20	-0.06

^aFor depictions of clusters, see Figure 5.

For Gd doping, there is a 0.02 eV barrier for Zn \rightarrow Gd electron hopping in $[\text{ZnGdO}_{10}]^{16-}$ while the Gd \rightarrow Zn barrier is 0.21 eV (Table 4). This is supported by calculations using the larger $[\text{Zn}_5\text{GdO}_{22}]^{32-}$ cluster where Gd does not trap. Rather, the electron delocalizes among all the metal atoms despite initially being localized on Gd during geometry optimization. The Zn \leftrightarrow Zn diabatic electron transfer barrier in the presence of Gd could not be computed since localized states are required. However, the delocalized state of the electron suggests the barrier may be nonexistent.

The behavior of Al also varies depending on the cluster model. When Zn and Al are face-sharing (in $[\text{ZnAlO}_{10}]^{16-}$), the electron localizes more favorably on Al than on Zn (by 0.09 eV; Table 4). As cluster size increases to $[\text{Zn}_5\text{AlO}_{22}]^{32-}$, Al does not trap at all. Instead, the localized electron is less stable on Al than on Zn by 0.52 eV. The Al \rightarrow $\text{Zn}_{\text{face-sharing}}$ barrier is much smaller (0.58 eV) than the $\text{Zn}_{\text{face-sharing}} \rightarrow$ Al one (1.10 eV). Attempts to localize the electron on $\text{Zn}_{\text{edge-sharing}}$ failed since it hopped from $\text{Zn}_{\text{edge-sharing}}$ to $\text{Zn}_{\text{face-sharing}}$ during the geometry

optimization. This precluded us from determining the effect of Al on $\text{Zn}_{\text{face-sharing}} \leftrightarrow \text{Zn}_{\text{edge-sharing}}$ electron transfer. Thus, Al forms a shallow trap in the small cluster and does not trap in the larger cluster.

For Y doping, the $\text{Y} \rightarrow \text{Zn}$ electron transfer barrier is 0.06 eV while the barrier for $\text{Zn} \rightarrow \text{Y}$ electron transfer is 0.48 eV. We also find the conduction electron delocalizes over all metal atoms despite initially localizing on a Zn atom during the geometry optimization (for $[\text{Zn}_5\text{YO}_{22}]^{32-}$; Figure S2). This further supports the conclusion that Y is a favorable dopant.

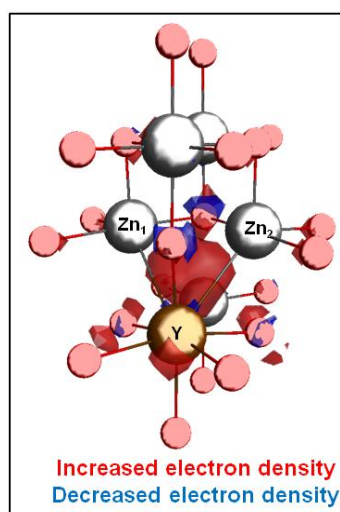


Figure S2: Density difference isosurface for an electron added to $[\text{Zn}_5\text{YO}_{22}]^{32-}$ with an isosurface value of 0.03 electrons/ \AA^3 . The difference is taken for the cluster density with the itinerant electron minus the cluster density without it; see text for details. Red (blue) indicates increased (decreased) electron density in the cluster with the electron relative to the cluster without it. Pink and white spheres denote O and Zn ions, respectively. This shows the delocalized distribution of the electron near Zn_1/Zn_2 and the Y dopant atom.

The $\text{Zn} \leftrightarrow \text{Zn}$ electron transfer barrier with F-doping was first studied using $[\text{Zn}_2\text{FO}_9]^{16-}$ (with F in the symmetric bridge or asymmetric positions; upper left of Figure 5). We also studied $[\text{Zn}_6\text{FO}_{21}]^{32-}$ (with F in the bridge position; lower left of Figure 5) for cluster size convergence. We compute a 0.05 eV barrier in $[\text{Zn}_2\text{FO}_9]^{16-}$ with F symmetrically-positioned. Calculations for larger clusters confirm these adiabatic features and show F-doping nearly eliminates the barrier. These trends initially suggest F is a highly attractive dopant (Figure 9

(b)). However, results derived from the cluster with F asymmetrically positioned in $[\text{Zn}_2\text{FO}_9]^{16-}$ show the electron prefers to localize on the Zn near F by 0.95 or 1.1 eV over the Zn farther away (Table 4 and Figure 9 (c)), which suggests instead that the electron will end up trapped near F.

F. Li-doped MnO:ZnO

We studied Li-doping of MnO:ZnO (Table S4) using the $[\text{Mn}_2\text{Zn}_3\text{LiO}_{22}]^{31-}$ cluster model (Figure S3). Barriers for hole transport along the $\text{Mn} \leftrightarrow \text{Mn}$, $\text{Mn} \rightarrow \text{O}_{\text{near}}$ pathways remain essentially unchanged with alloying (Table S4). The $\text{O}_{\text{near}} \leftrightarrow \text{O}_{\text{far}}$ and $\text{Mn} \rightarrow \text{O}_{\text{far}}$ hole transport barriers are also very similar for the two materials with less than 0.1 eV difference. The $\text{O}_{\text{far}} \rightarrow \text{Mn}$ barrier exhibits the largest change increasing by 0.18 eV with alloying. Overall, the relative energetics for hole transport in Li-doped MnO:ZnO remain similar to hole transport in Li-doped MnO.

Material (cluster model)	$\text{Mn} \leftrightarrow \text{Mn}$	$\text{O}_{\text{near}} \rightarrow \text{O}_{\text{far}}$ $\text{O}_{\text{far}} \rightarrow \text{O}_{\text{near}}$	$\text{Mn} \rightarrow \text{O}_{\text{far}}$ $\text{O}_{\text{far}} \rightarrow \text{Mn}$	$\text{Mn} \rightarrow \text{O}_{\text{near}}$ $\text{O}_{\text{near}} \rightarrow \text{Mn}$
Li-doped MnO $[\text{Mn}_5\text{LiO}_{22}]^{32-}$	0.82	0.46 0.37	0.60 0.48	0.27 0.42
Li-doped MnO:ZnO $[\text{Mn}_2\text{Zn}_3\text{LiO}_{22}]^{31-}$	0.83	0.53 0.45	0.52 0.66	0.25 0.47

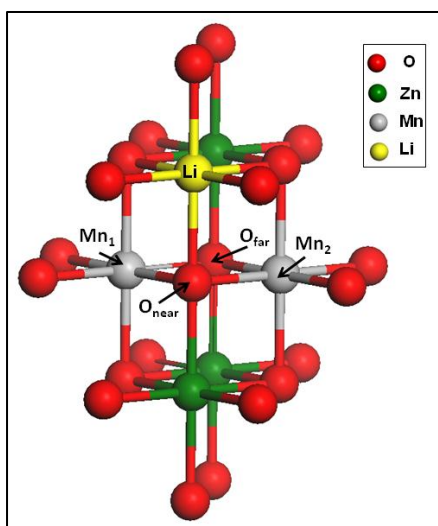


Figure S3: $[\text{Mn}_2\text{Zn}_3\text{LiO}_{22}]^{3-}$ cluster used to model hole transport in Li-doped MnO:ZnO.

G. Hole transfer in undoped MnO and MnO:ZnO

The diabatic curves for Mn \leftrightarrow Mn and O \leftrightarrow O hole transfer in various embedded clusters modeling undoped MnO or MnO:ZnO are shown in Figure S4. The barrier changes very little and the curves lie essentially on top of one another (except in one asymmetric hole transfer case).

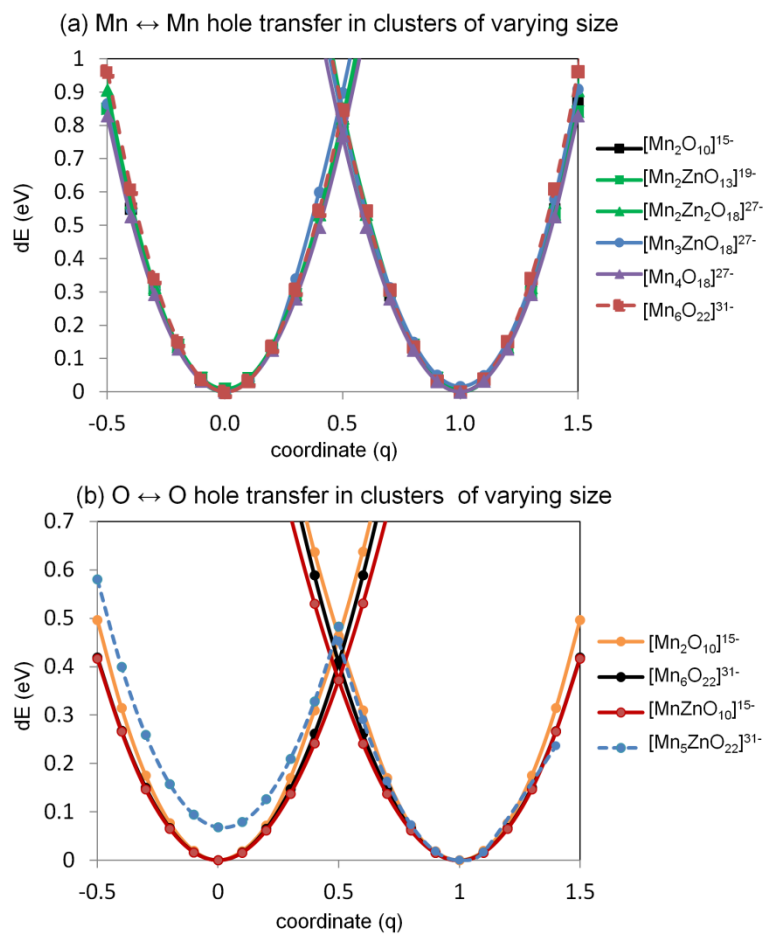


Figure S4: Hole transfer along the (a) Mn \leftrightarrow Mn and (b) O \leftrightarrow O pathways in undoped MnO and MnO:ZnO